Investigating Ramp Wave Propagation inside Silica Glass with Laser Experiments and Molecular Simulations

R. Renou[1], L. Soulard[1], E. Lescoute[1], C. Dereure[2], M. Nivard[2], J. Sangleboeuf[2], D. Loison[2], J. Guin[2], L. Berthe[3]

Under elastic shock compression silica glass exhibits a very specific behaviour. A shock propagating inside a material is usually seen as the propagation of a discontinuity. However in silica glass, shocks are unstable and lead to the propagation of a ramp wave where the shock front becomes gradually larger over time. Ramp waves were already reported in the literature, however their origin remain uncertain. This work presents an original study combining laser shock-induced experiments and molecular dynamics simulation aiming to improve the understanding of the mechanisms involved. Experimental ramp waves were directly observed using shadowgraphy technique allowing for an estimation of the head and tail velocities. Molecular dynamics simulations were carried out in order to reproduce ramp waves and to gain insight into the material properties. Ramp waves were observed for both elastic and plastic shockwaves. In the latter case, the plastic waves were preceded by an elastic ramp precursor. The sound speed, related to the material compressibility, was found to decrease with increasing pressure, as observed experimentally for quasi-static hydrostatic loading, thus providing an explanation for the instabilities that lead to the propagation of ramp waves.

Silica (SiO_2) is one of the most common minerals on earth. Although this material is usually encountered in one of its numerous allotropic crystallized form, a vitreous phase referred as silica glass may be synthesized by rapid quenching of the molten material. Silica glass, in its high purity form, is used primarily for its optical properties, in light transmission, high resolution micro-lithography, or in high intensity laser optics. Regarding the present scientific case of this study, silica glass presents two major interests: on the one hand, the chemical structure is simple and made of only two atoms (Si and O) making the synthesis easier; on the other hand, silica glass presents a specific atomistic organization resulting in anomalous thermomechanical properties compared with other glassy materials. For instance, under hydrostatic compression, the bulk modulus was shown to reach a minimum value near 2 to 3 GPa (Meade and Jeanloz (1987)) before increasing with pressure as observed in most materials.

In order to get a better understanding of the shock behaviour of such an anomalous material a series of laser shock experiments were carried out using the ELFIE facility at the Laboratoire d'Utilisation des Lasers Intenses (LULI), at the French École Polytechnique. These laser shots consisted in focusing a laser impulse on a 1.27 mm focal spot on the front surface of the sample. The ELFIE laser source has the following characteristics: a 1057 nm wavelength and energy up to 10 J with a 350 fs impulse or up to 50 J with a 600 ps impulse. The shocked samples consisted in 10x10 mm parallelepipeds of fused silica (spectrosil®2000) with a thickness comprised between 1.5 and 3 mm. The samples were polished down to the micron on four out of six sides to have sufficient transparency for shadowgraphy instrumentation purposes. A few μm thick aluminum layer was deposited on the front face of the samples in order to obtain a controlled and known laser-matter interaction. This interaction produces a plasma that expands rapidly thus generating a shockwave that propagates into the sample. After the laser pulse, a release wave starts to propagate in the sample in the same direction as the initial shock wave. In order to avoid any laser breakdown the sample was placed in a vacuum chamber. The optical index changes because the shockwave propagates into the sample resulting in contrast variation that can be observed through visualization methods, as described by Hall (1982) and Ecault et al. (2015). In our work, the experimental setup comprised notably a time-resolved shadowgraphy apparatus composed of a high-speed camera focused on the sides of the sample and illuminated by a continuous laser, as described in a previous publication (Renou et al. (2017)).

The two shadowgraphy pictures, Figure 1.a and Figure 1.b, were taken respectively at 150 ns and 300 ns after the laser shot. In this specific shot the laser flux was 8.4 TW/cm^2 corresponding to an estimated pressure of 184 GPa, computed by simulations with the ESTHER code (Colombier et al. (2005), Bardy et al. (2017)). The first picture shows only one visible shockwave front, pinpointed by both black and white arrows. On the other hand, the second

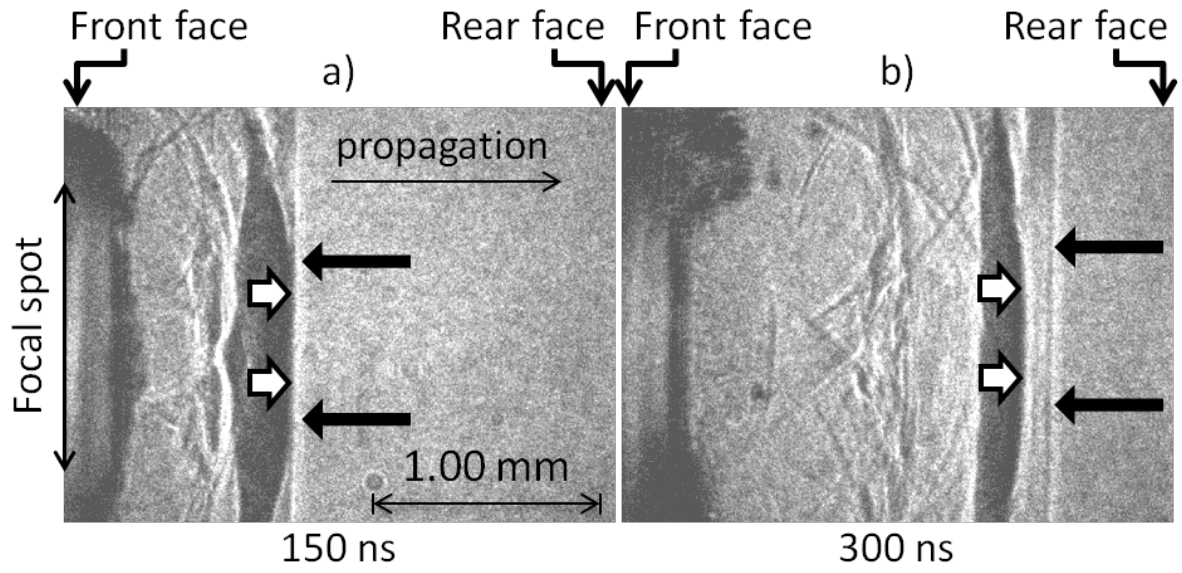

Figure 1: Time-resolved shadowgraphy pictures taken from the side of a silica sample during a laser-shock experiment with a 600 ps laser impulse and a 8.409 TW/cm^2 flux. The front face is located on the left side of the pictures and the shock propagates from left to right. These pictures were respectively taken 150 and 300 ns after the shot. Arrows indicate the location of the primary and secondary shock front respectively in black and white.

picture presents a shock front separated in two fronts as indicated by the gap between the arrows.

This separation into two waves is observed when the shockwave is unstable. This phenomenon usually occurs when the material experienced strong structural changes, like a phase transition or permanent deformation (plasticity). In the latter case, the slower plastic wave is preceded by a faster elastic wave called precursor. The limit between an elastic behaviour and a plastic+precursor behaviour is called the Hugoniot Elastic Limit (HEL), corresponding to a shock pressure of 8 GPa for silica glass (Sugiura et al. (1981)). However, several studies made on silica glass reported a slightly different phenomenon (Alexander et al. (2008), Chhabildas and Grady (1984), Sugiura et al. (1981)). In these studies silica glass did not display the traditional elastic precursor - plastic shock behaviour with an abrupt increase of the particle velocity behind shock waves. Instead, both elastic and plastic waves were preceded by a ramp where both the velocity and the pressure gradually increase, as illustrated in Figure 2. In our case the shockwave was already attenuated when the pictures of Figure 1 were taken. The release wave caught up with the compressive shock wave and started to gradually diminish the shock pressure. At 150 ns the shock pressure is below the HEL, and therefore the observed waves are likely to be elastic waves.

In order to investigate this particular phenomenon in silica glass, non-equilibrium molecular dynamics simulations were performed to simulate a shock propagation inside the material. A mobile piston with a given high velocity was used to impact the sample and generate a 1D shock. The sample is of size 14x14x1200 nm, about 10 million atoms, long enough to catch all mechanisms involved. The CHIK model was chosen to reproduce the silica behaviour (Carré et al. (2008)). In a recent study this potential was indeed proved to give a reliable description of silica glasses under shock loading conditions (Renou et al. (2017)). The simulations ran in the microcanonical ensemble (NVE) during 150 ps. All simulations were realized with Stamp developed by the French Commissariat à l'Énergie Atomique, CEA. Additional details on the methodology are available in our previous work (Renou et al. (2017)).

In this present study, several simulations were carried out with different material velocities between 150 m/s to 3000 m/s corresponding to shock pressures up to 40 GPa. Figures 3.a, 3.b, 3.c and 3.d illustrate four shock fronts obtained in simulations with initial velocities of 150 m/s (3 GPa), 500 m/s (7 GPa, just below the HEL), 2000 m/s (23 GPa) and 2500 m/s (37 GPa) respectively. The shock front shapes are very different depending on the shock pressure considered. Two shock front velocities were calculated: the "head" and the "tail" velocities computed at $u_p = 0.8u_{p0}$ and $u_p = 0.2u_{p0}$ according to Su et al. (2014). A ramp wave is observed for the lowest shock pressure, Figure 3.a. A slight delay is observed between the head and the tail of the ramp but they both propagates at a the same velocity of 6272 m/s. The ramp wave is stable over time. At 7 GPa, Figure 3.b, a decaying ramp wave is observed. The head is propagating at 6317 m/s but the tail is about 10% slower propagating at 5765 m/s. This difference between head and tail induces a particular front that progressively becomes wider over time. For the

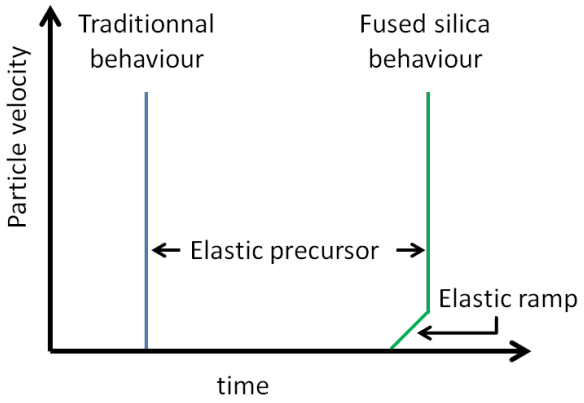

Figure 2: Evolution of the particle velocity over time inside a solid material. Comparison between a traditional shock behaviour (left, blue curve) and the shock behaviour of fused silica (right, green curve). In the traditional shock behaviour both elastic and plastic waves generate a brutal increase of pressure and particle velocity. In fused silica both are preceded by a ramp where pressure and particle velocity gradually increase.

shock pressure of 23 GPa, above the HEL, Figure 3.c, the shock front corresponds to a plastic wave with an elastic precursor as described in the previous section. The plastic front propagates at a constant velocity of 3088 m/s. The elastic precursor is a decaying wave similarly to the 7 GPa case. The head of the precursor is propagating at 4232 m/s. Finally, for the highest pressure of 37 GPa, Figure 3.d, the elastic precursor is barely visible and the plastic wave propagates at a constant velocity of 3403 m/s.

Two shock velocities were extracted from the shadowgraphs. In Figure 1.b, the head velocity (black arrows) was estimated at 5921 m/s and the tail (white arrows) propagates 14.5% slower, at 5063 m/s. The simulations give slightly different velocities as already reported by Wang et al. (2015) and Su et al. (2014). These authors both reported similar decaying ramp waves for an initial velocity of 500 m/s (around 7 GPa) with the Tersoff potential of Munetoh et al. (2007). Su et al. (2014) computed a head and tail velocity of 5.6 and 4.2m/s for a 500 m/s shock. The Munetoh potential is however known to fail to reproduce several key properties of silica glasses (Cowen and El-Genk (2015)). An additional simulation was carried out to reproduce an unsteady shock propagation. In this case, a silica projectile hits the silica glass target at high velocity generating two compressive waves that propagate in both the projectile and the sample. The wave traveling in the projectile bounces back at the front face turning into a faster rarefaction wave that catches up with the compressive wave propagating in the sample. The resulting shock front is shown Figure 4. The simulation was designed to reproduce the experimental laser shot with a particle velocity of 511 m/s and a maximum shock pressure of 5.61 GPa. The left part of the shock front shows the rarefaction wave getting closer to the compressive wave. The right part shows a slowly decaying compressive front similarly to what was observed in Figure 3.b. The head velocity was estimated at 6265 m/s and the tail velocity is 15.6% slower at 5287 m/s. The molecular dynamics simulations seem to overestimate the shock velocities. However the ratio between head and tail velocities are identical. The simulation is in qualitative agreement with the experiments There are natural discrepancies between molecular dynamics and experimental results due to the nature of molecular simulations. For example, the quality of the model used may impact the results, and the space and time available by simulations are far behind the experimental scales. Despite the limitations of molecular dynamics simulations, ramp waves are fairly well reproduced and are in a qualitative agreement with experiments. Molecular dynamics simulations can be used to investigate the structural properties and improve the understanding of complex dynamic processes in silica glasses.

For the present case, the presence of an elastic ramp can be explained by a decrease of the sound velocity in the shocked silica glass behind the shock wave. The bulk sound speed c in a material can be extracted from isentropic compression, Equation 1.

$$c^2 = \left(\frac{\partial P}{\partial \rho}\right)_s \tag{1}$$

P and ρ are the pressure and density respectively. The bulk sound speed is a property available in molecular simulations. We choose here to use the Hugoniostat method where the motion equations are rewritten so the system naturally converge toward shocked states (Maillet and Stoltz (2008)). Successive compressions using

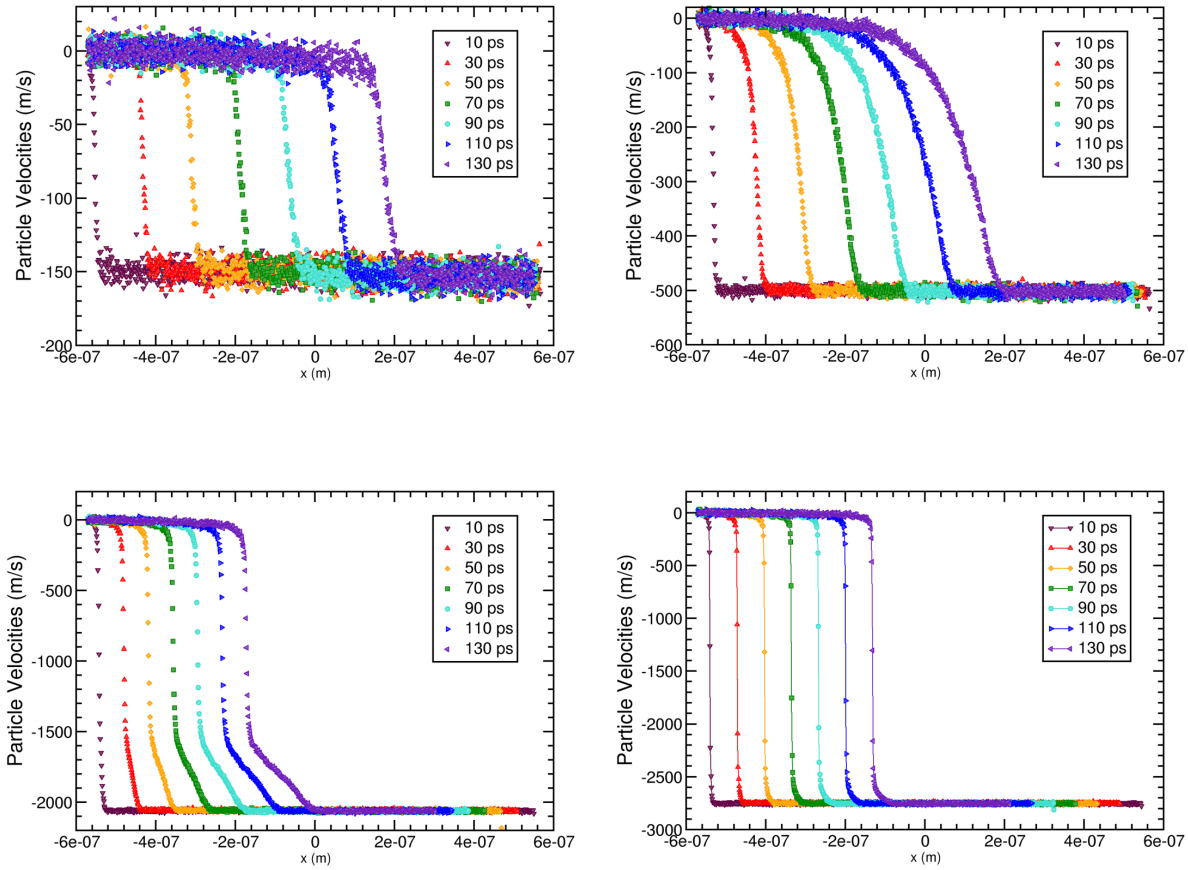

Figure 3: Shock front obtained with molecular dynamics simulations at different shock pressures. a) A ramp wave is observed for a shock pressure of 3 GPa. b) A shock pressure of 7 GPa induces a decaying ramp wave. c) Above the HEL of 8GPa, a plastic wave with an elastic precursor is observed for a shock pressure of 23 GPa. d) Above 37 GPa, the elastic precursor is not visible anymore.

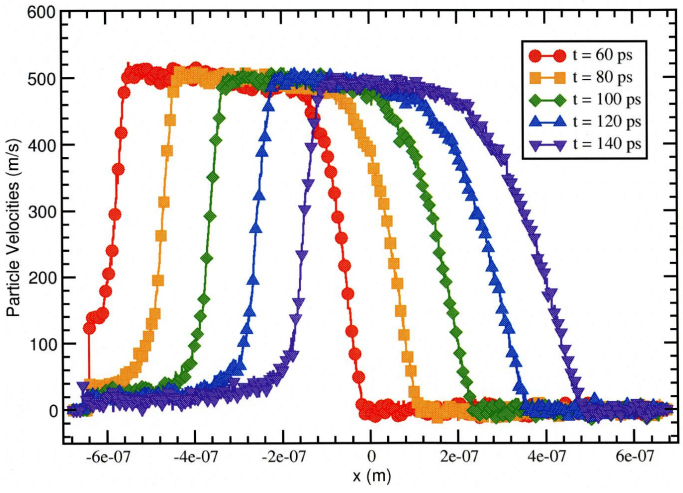

Figure 4: Unsteady shock propagating in the silica glass sample. The simulation was designed to match the experimental laser shot conditions. The particle velocity was estimated at 511 m/s and the maximum shock pressure at 5.6 GPa.

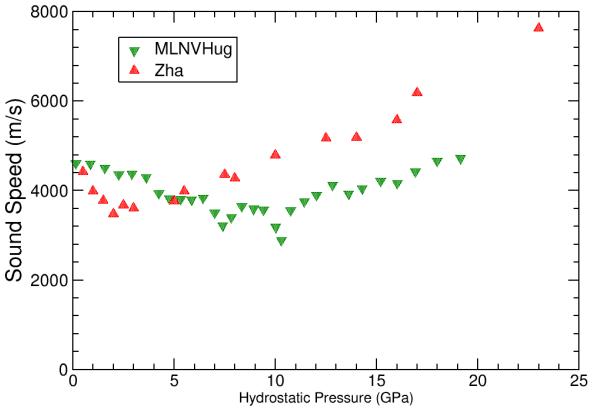

Figure 5: Evolution of the silica bulk sound speed with pressure. Comparison between numerical and experimental data (Zha et al. (1994)).

the Hugoniostat method are isentropic and the sound speed computation is therefore more accurate than in the microcanonical or canonical (NVE, NVT) ensemble. One other advantage with the Hugoniostat method lies in the low computational cost. Small systems composed of 24 000 atoms are sufficient to reproduce adequately shocked states in silica glass materials (Renou et al. (2017)). Every successive compressions consisted in this work in 100 ps of equilibration and 100 ps of data acquisition.

The evolution of the sound speed with pressure is shown in Figure 5. Experimental data obtained from Brillouin scattering obtained under hydrostratic compression are also reported (Zha et al. (1994)). In spite of clear differences, the numerical and experimental curves show the same trend. A local minimum is observed experimentally at 3 GPa and 12 GPa by simulation. Molecular dynamics simulations highly depends on the quality of the model used. The CHIK potential is known to fairly well reproduce the shock behavior of silica. However, under hydrostatic compressions, this potential fails to reproduce several properties and some other model may behave better under compression. This fact does not change the conclusion. The decreasing sound speed with pressure can still be correlated to the shock front shapes. Under shock-loading, a local minimum observed on the bulk sound speed curve causes the elastic domain of the Hugoniot curve to be bended instead of being linear, as shown in Figure 6. In this graph, the line linking the initial state and the shocked state is called the Rayleigh line. The shock is unstable if the Rayleigh line crosses the Hugoniot curve, causing the separation of the initial wave into several shockwaves (Meyers (2007)). In a traditional material (Figure 6.b) shocked state 3 can directly be reached from state 0 because the Rayleigh line (in red) does not cross the Hugoniot curve. In silica glass in the case of a bent Hugoniot curve (Figure 6.a) the same state 3 cannot be reached directly as previously but instead intermediate states 1 and 2 have to be reached before jumping at 3. The compressive wave is no longer a shockwave in this case but a ramp wave.

In our experiments, presented on Figure 1.a, the shockwave is caught up with the release wave, leading to a gradually decrease of the shock pressure. At a certain point the shocked state will reach a level that cannot be reached through a direct Rayleigh line linking it to the initial state, as described in Figure 6.a, as a result the wave will become unstable. However, because the Hugoniot curve of silica is bended in the elastic domain, the shocked state cannot be reached by only two separate waves as it usually does. The instability will instead generate a ramp formed by a succession of equilibrium states. The maximal pressure reached in this ramp wave is likely to be only a few GPa, because between the first and second fronts in Figure 1.b the shade of the grey area is not very different from the shade of the unaffected silica (on the right of the primary front).

In order to conclude, the propagation of ramp waves in silica glass was studied in this work. Despite several recent studies, ramp waves are still misunderstood and difficult to study by experimental means. This work reports both laser experiments and molecular simulations on this phenomenon occurring in silica glasses. Experimental ramp waves propagating inside the material were directly observed with a shadowgraph technique. In addition, molecular dynamics simulations were performed in order to probe the microscopic properties. Numerical ramp waves were obtained in both the elastic and plastic regime. The head and tail velocities were in a fair agreement with experiments. The material properties were computed and the speed of sound was found to anomalously decrease with pressure. The Hugoniot curves showed a negative curvature indicating the propagation of unstable

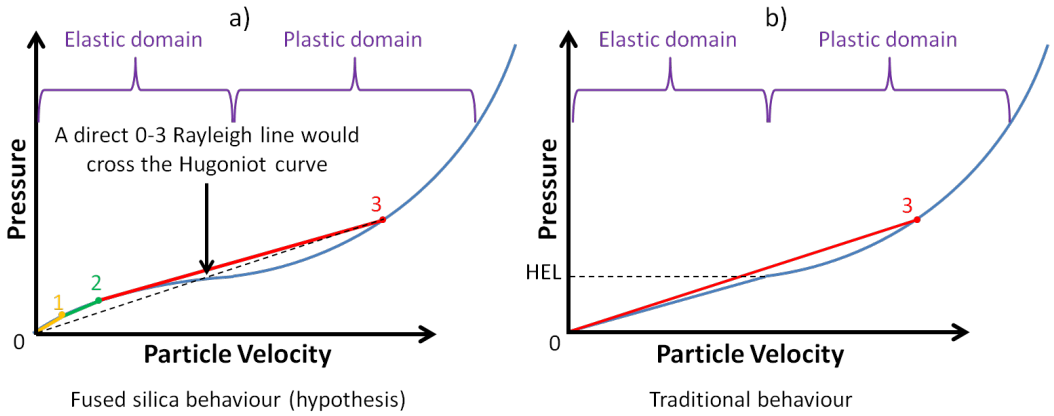

Figure 6: The bending of the fused silica Hugoniot, curve a), could lead to widening the wave front by opposition to a traditional Hugoniot, curve b). To reach state 3, silica has to pass through states 1 and 2, because the Rayleigh line would otherwise cross the Hugoniot curve. A Rayleigh line crossing the Hugoniot curve is the sign of unstable shocks (Meyers (2007)).

elastic shockwaves and elastic precursors in the case of plastic loading conditions. The plastic behaviour of silica glass under hydrostatic compressions and shock loading conditions will be investigated in a future work.

Acknowledgment

This work has been carried out thanks to the joint access between CNRS and CEA to the LULI National facility. The authors are also grateful to the French Agence Nationale de la Recherche for its financial support through the program ANR GLASS (ANR-14-CE07-0020).

References

Alexander, C. S.; Chhabildas, L. C.; Reinhart, W. D.; Templeton, D. W.: Changes to the shock response of fused quartz due to glass modification. *Int. J. Impact Eng.*, 35, 12, (2008), 1376–1385.

Bardy, S.; Aubert, B.; Berthe, L.; Combis, P.; Hébert, D.; Lescoute, E.; Rullier, J.-L.; Videau, L.: Numerical study of laser ablation on aluminum for shock-wave applications: development of a suitable model by comparison with recent experiments. *Optical Engineering*, 56, 1, (2017), 011014–011014.

Carré, A.; Horbach, J.; Ispas, S.; Kob, W.: New fitting scheme to obtain effective potential from car-parrinello molecular-dynamics simulations: Application to silica. *Europhys. Lett.*, 82, 1, (2008), 17001.

Chhabildas, L.; Grady, D.: Shock loading behaviour of fused quartz. In: J. ASAY; R. GRAHAM; G. STRAUB, eds., *Shock Waves in Condensed Matter 1983*, pages 175 – 178, Elsevier, Amsterdam (1984).

Colombier, J. P.; Combis, P.; Bonneau, F.; Le Harzic, R.; Audouard, E.: Hydrodynamic simulations of metal ablation by femtosecond laser irradiation. *Phys. Rev. B*, 71, (2005), 165406.

Cowen, B. J.; El-Genk, M. S.: On force fields for molecular dynamics simulations of crystalline silica. *Comput. Mater. Sci.*, 107, (2015), 88–101.

Ecault, R.; Berthe, L.; Touchard, F.; Boustie, M.; Lescoute, E.; Sollier, A.; Voillaume, H.: Experimental and numerical investigations of shock and shear wave propagation induced by femtosecond laser irradiation in epoxy resins. *Journal of Physics D: Applied Physics*, 48, 9, (2015), 095501.

Hall, K.: Observing ultrasonic wave propagation by stroboscopic visualization methods. *Ultrasonics*, 20, 4, (1982), 159–167.

Maillet, J.-B.; Stoltz, G.: Sampling constraints in average: The example of hugoniot curves. *Appl. Math. Res. Express*, abn004.

Meade, C.; Jeanloz, R.: Frequency-dependent equation of state of fused silica to 10 gpa. *Phys. Rev. B*, 35, (1987), 236–244.

Meyers, M. A.: *Dynamic Behavior of Materials*. John Wiley & Sons, Inc. (2007).

Munetoh, S.; Motooka, T.; Moriguchi, K.; Shintani, A.: Interatomic potential for si–o systems using tersoff parameterization. *Computational Materials Science*, 39, 2, (2007), 334–339.

Renou, R.; Soulard, L.; Lescoute, E.; Dereure, C.; Loison, D.; Guin, J.-P.: Silica glass structural properties under elastic shock compression: Experiments and molecular simulations. *The Journal of Physical Chemistry C*, 121, 24, (2017), 13324–13334.

Su, R.; Xiang, M.; Chen, J.; Jiang, S.; Wei, H.: Molecular dynamics simulation of shock induced ejection on fused silica surface. *J. Appl. Phys.*, 115, 19, (2014), 193508.

Sugiura, H.; Kondo, K.; Sawaoka, A.: Dynamic response of fused quartz in the permanent densification region. *J. Appl. Phys.*, 52, 5, (1981), 3375–3382.

Wang, J.; Rajendran, A.; Dongare, A.: Atomic scale modeling of shock response of fused silica and α-quartz. *J. Mater. Sci.*, 50, 24, (2015), 8128–8141.

Zha, C.; Hemley, R. J.; Mao, H.; Duffy, T. S.; Meade, C.: Brillouin scattering of silica glass to 57.5 gpa. *AIP Conference Proceedings*, 309, 1, (1994), 93–96.

Address:
[1] CEA, DAM, DIF, 91297 Arpajon, France
[2] Institut de Physique de Rennes - UMR CNRS 6251, 263 Avenue Général Leclerc, Université de Rennes 1, 35700 Rennes, France
[3]PIMM, CNRS-ENSAM Paritech, 151 Boulevard de l'Hopital, 75013 Paris Cedex, France
email: `richard.renou@cea.fr`